Management of Swirling Flows with Application to Wind Tunnel Design

R. A. Wigeland,* M. Ahmed,† and H. M. Nagib‡
Illinois Institute of Technology, Chicago, Ill.

The effect of various flow manipulators on different types of swirling flows was investigated experimentally in order to determine the important mechanisms involved and to gain insight into efficient means for removing such swirls from wind tunnels and duct flows. Several swirling test flow conditions were used which had different transverse distributions of angular momentum and turbulence intensity levels. They represented typical conditions arising in flows through ducts and wind tunnels. The effectiveness of commonly used flow manipulators, such as screens, grids, and honeycombs, in removing the swirl from these flows was established. Different mechanisms dominated depending upon the scaling between the swirl size and the characteristic lengths of the manipulator, with some mechanisms being more efficient in removing the swirl than others. In many cases, similar performance was obtained by any one of several manipulators, making it possible to select a flow manipulator based on other criteria, such as maximum turbulence suppression or minimum pressure drop, which are both very important in wind tunnel design and operation.

Nomenclature

b_i = full width of vortex based on absence of vane-vorticity indicator rotation along i direction
Δb = percentage difference between width of vortex along two perpendicular transverse directions
K = pressure drop coefficient of turbulence manipulator $= \Delta P/(\rho U_\infty^2/2)$
ℓ = length of turbulence manipulator in streamwise direction
M = mesh length or distance between openings of turbulence manipulator
N_v = angular velocity of vane-vorticity indicator in rpm, proportional to local streamwise vorticity
Re_M = Reynolds number based on turbulence manipulator mesh size $= U_\infty M/\nu$
U_∞ = freestream mean velocity
x = axial or streamwise distance
y = lateral distance normal to streamwise direction and measured from center of test section
z = vertical distance normal to streamwise direction and measured from center of test section
α = half-angle setting between airfoils
σ = solidity of turbulence manipulator; equal to solid area divided by total cross-sectional area normal to flow

I. Introduction

IN order to perform quality wind tunnel experiments, it is necessary to establish a flow through the test section which has certain known and desirable characteristics, such as a uniform freestream velocity profile and low-turbulence intensity level. In addition, all secondary or swirling motions should be removed from the flow. These secondary motions arise from a number of sources in wind tunnels. For example, the fan which provides the flow through the tunnel, any corners and bends, flow separation, or the intake conditions of open return wind tunnels can all create secondary motions. When testing helicopter and V/STOL models, the models themselves generate swirls and downwash which in turn create rotational nonuniformities. Such motions subside very slowly around the tunnel circuit and contaminate the flow coming into the test section. The solution of this problem is frequently an empirical method relying on ingenuity rather than on well-established methods. Often this results in "overkilling," or the inefficient use of honeycombs, screens, and other flow manipulators which leads to losses in tunnel performance, such as a decrease in the maximum flow velocity. For these reasons, experiments were performed to determine the effect of standard flow manipulators on various types of swirling flows and to discover the mechanisms by which the manipulators operated on the swirling flow. From this information, the proper manipulators can be selected and used in an efficient scheme for improving the flow characteristics of the wind tunnel or duct.

A considerable amount of theoretical and experimental information is available on the effects of various flow manipulators on turbulence and mean velocity nonuniformities. For a detailed discussion of the literature, the reader is referred to the report by Loehrke and Nagib.[1] It is important to point out that all the available theoretical studies assume that the incoming turbulence is isotropic and homogeneous, while the experimental investigations are primarily concerned with the details of the effects of screens on grid-generated turbulence. Limited information is available on the effects of flow manipulators on mean velocity components which are not perpendicular to the entrance plane of the device. However, these discussions are restricted mainly to screens, where the deflection of the flow was found to be related to the pressure drop coefficient; e.g., see Taylor and Batchelor,[2] Dryden and Schubauer,[3] and Laws and Livesey.[4] Although both theoretical and semiempirical attempts have been made to establish the exact form of this relationship, no entirely satisfactory form has been developed. In practice, long, fine mesh honeycombs and turning vanes have been the primary elements used as means of removing secondary flows and swirl from wind tunnels and ducts. However, as demonstrated by Loehrke and Nagib[1] for the case of nonuniformities in the mean flow, using the pressure drop alone across the manipulator is an inefficient method of controlling the flow

Presented as Paper 77-585 at the AIAA/NASA Ames V/STOL Conference, Palo Alto, Calif., June 6-8, 1977; submitted June 15, 1977; revision received May 30, 1978.

Index categories: Research Facilities and Instrumentation; Simulation; Viscous Nonboundary-Layer Flows.

*Visiting Assistant Professor.
†Graduate Assistant; presently with Abbott Laboratories, North Chicago, Ill.
‡Associate Professor. Member AIAA.

characteristics since it ignores the possibility of other mechanisms. Some of these mechanisms may be nonlinear in nature and very effective.

For any experiment to evaluate accurately the operation of passive flow manipulators in the control and management of flows, the test flow conditions must have known characteristics controllable over a wide range of parameters. In this study, the approach established in our earlier work[1,5] on management of freestream turbulence was followed. The test flows which contain swirling components were established and documented over a range of conditions. The effect of inserting any flow manipulator was then determined by comparing the resulting flow with the original test flow condition. Detailed measurements provided information about the mechanisms by which such flow manipulators remove or change the swirl or secondary motion.

II. Experimental Approach

These experiments were performed in the facility schematically represented in Fig. 1. An open-circuit wind tunnel was used to facilitate complete probing of the flow downstream of the swirl generator and flow manipulator. The test section was assembled from various lengths of 6-in.-diam plexiglas tube or duct. The swirl generators were constructed using similar sections of plexiglass tube which allowed them to be incorporated as part of the test section assembly. The flow manipulators were designed to permit their installation either in one of the sections or between two sections. These features provided great flexibility in changing the swirl generators and flow manipulators or in altering their respective positions.

A. Flow Manipulators

In order to achieve the objectives as stated in Sec. I, it was necessary to have a wide variety of flow manipulators to study so that any trends in their performance could be determined and the underlying physical mechanisms established. The manipulators used and their physical dimensions are given in Table 1. They represent a range of mesh sizes M, solidities σ, and lengths ℓ for several types of manipulators. Another important operating characteristic for any flow manipulator is its pressure drop coefficient since it is directly related to any decrease in the maximum flow velocity of the facility in which it is incorporated. The pressure drop coefficients for the manipulators described in Table 1 are shown as a function of velocity in Fig. 2. An additional consideration is the suppression or generation of turbulence by the manipulator because controlling the turbulence level is just as crucial for wind-tunnel testing as removing any swirling or secondary flow. However, since Loehrke and Nagib in their recent work[1,5] provide a large amount of information on the management and control of turbulence, the present study deals primarily with the aspect of removing the swirling and secondary flows. Any additional turbulence generated by the manipulator which is due to the incoming secondary motion can be handled with the aid of the information contained in Refs. 1 and 5.

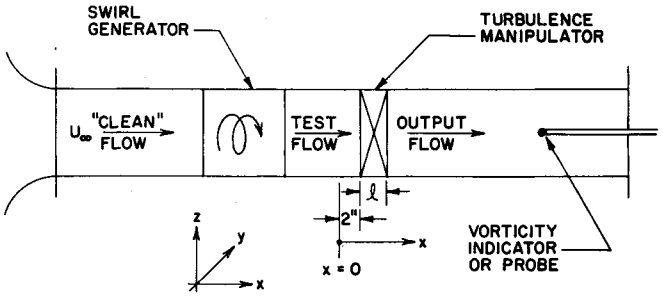

Fig. 1 Schematic of test section arrangement for swirl management investigations.

B. Generation of the Test Flows

Several different swirl generators were used to develop various types of rotational flows representing a wide range of swirling conditions. The airfoil swirl generator consists of two adjacent airfoils, each spanning half the test section and set at equal but opposite angles of attack α. This generator superimposes a concentrated vortex located in the center of the test section on the flow through the test section. This arrangement resulted in swirling flow conditions that had all of the vorticity concentrated in a region near the center of the duct, with the remaining flow being essentially irrotational. These flow conditions also changed very little with downstream distance. Both the freestream velocity and angle of attack were varied to obtain vortices covering a range of strengths and sizes.

Another swirl generator, called the tangential-jet swirl generator, consists of eight tangential jets equally spaced around the periphery of one of the ducts. All of the angular momentum in these test flow conditions was confined to a region near the walls, and the majority of the test section flow was relatively unaffected. For this generator, the freestream velocity and jet velocity were varied over a range of values to obtain different test flow conditions.

The third swirl generator, called the swirling-jet ejector, consisted of a jet with an adjustable rotational component exiting along the axis in the center of one of the ducts. In this case, the remainder of the flow was provided by the entrainment action of the jet and not by a separate blower as in previous cases. This resulted in a flow having most of the angular momentum near the center of the duct. However, unlike the first case of the concentrated vortex, the jet spread rapidly with downstream distance distributing the angular momentum over a larger part of the flow. To generate different flow conditons using this swirl generator, the jet velocity and amount of rotation were varied.

Using suitable choices of the settings possible with each swirl generator, the test flows indicated in Fig. 1 were established. Further details about the construction and calibration of these swirl generators are included in a report by Ahmed et al.[6]

C. Instrumentation

Since all of the resulting test flows involved rotational components, a convenient means for their direct measurement

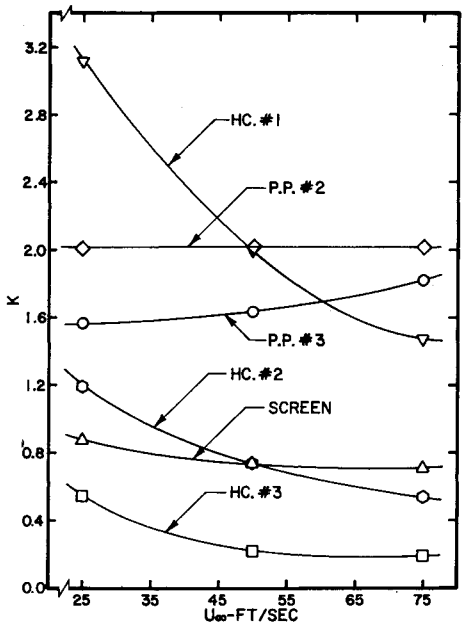

Fig. 2 Pressure drop coefficient of manipulators vs freestream velocity.

was necessary. One method used extensively for this investigation is the vane-vorticity indicator. The vanes used in this investigation were improved versions of that used by Holdeman and Foss.[7] Similar devices have been used for vorticity measurements by McCormick et al.,[8] Barlow,[9] and more recently, Zalay.[10] Briefly, a vane is described as four perpendicular blades which are at zero angle of attack to the nonrotating flow. The vane is able to rotate about its axis, which coincides with the junction of the four blades along the streamwise direction. Such a vane will not rotate in parallel flows, but will when there is a rotational component in the streamwise direction. Calibration showed that the rotation of the vane could be directly related to the streamwise vorticity in the flow. However, due to bearing friction in the vane, there is a threshold of rotation. In some cases, the vane will indicate that all of the vorticity has been removed when there is some small residual vorticity in the flow. Details of the calibration and construction can be found in Ahmed et al.[6,11]

In addition to the vane-vorticity indicator, standard hot-wire and X-wire probes were used. In particular, X-wire probes were used to document the details of the mechanisms present, to investigate in more detail conditions which remained unexplained by the vane-vorticity measurements alone, and to obtain some information on the turbulence in the flow.

D. Test Flow Conditions

A wide variety of test flow conditions was established for the three swirl generators. These test flows were documented by measuring the streamwise vorticity downstream of each generator when no turbulence manipulator was present in the duct. For example, the downstream development of some of the airfoil test flow conditions is given in Fig. 3. These conditions are generally classified using "V" followed by a number, with a larger number indicating a stronger vortex. The vane is positioned in the center of the wing tip vortex and x is measured from the trailing edge of the airfoils. The almost constant vane rotational speed N_v supports the earlier statement that these flow conditions change very little with downstream distance. The reason for selecting these particular conditions, which cover several freestream velocities and airfoil angles of attack, was to have test flow conditions with 1) the same vortex strength but different sizes, V-2-1 and V-2-2, 2) the same freestream velocity with different vortex sizes and strengths, V-3 and V-4 or V-1 and V-2-2, and 3) the same vortex size for several freestream velocities, V-1, V-2-1, and V-4. Using such conditions, the effects of these parameters on the manipulator operation was evaluated.

Further details on these flow conditions are given in Fig. 4. In the top part of the figure, the symmetry of the vortices is demonstrated for one test flow condition by the agreement between horizontal and vertical profiles of vorticity. More complete information is listed in the lower part of Fig. 4, where the vortex widths b_y and b_z in the horizontal and vertical directions, respectively, are given for five flow conditions. The value Δb is a measure of the asymmetry of the vortices, which was small for every case, as indicated by the values given in Fig. 4.

A variation on these test flow conditions is presented in Fig. 5. Using the same freestream velocity and airfoil angle of attack as listed in Fig. 3, a grid was placed upstream of the airfoils to generate additional background turbulence. For example, flow condition V-2-1 became $(V\text{-}2\text{-}1)_T$ when the grid was in place. While the extra turbulence generally reduced the strength of the vortex slightly, it did not cause the vortex to decay any faster with downstream distance than in the lower turbulence case. Therefore, these flow conditions were useful for establishing the effect of background turbulence level on manipulator operation.

III. Results and Discussion

Using the preceding test flow conditions along with the various flow manipulators, measurements were made in the

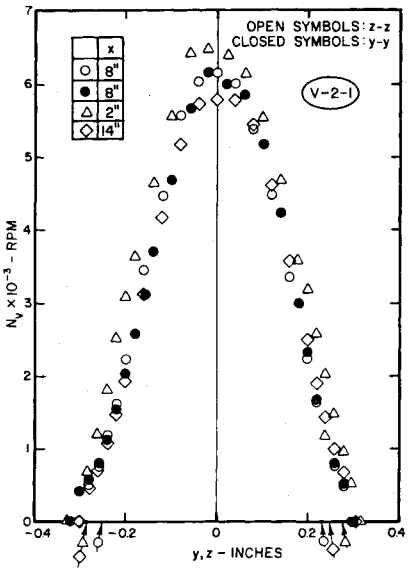

x = 8 IN.			
FLOW CONDITION	b_y IN.	b_z IN.	$\Delta b = \lvert b_y - b_z \rvert / \frac{(b_y + b_z)}{2}$
V-1	0.82	0.83	1%
V-2-1	1.06	0.98	8%
V-2-2	1.56	1.51	3%
V-3	0.82	0.86	5%
V-4	1.22	1.34	9%

Fig. 4 Horizontal and vertical distributions of vorticity indicator rotation in test flow condition V-2-1 and vortex sizes in test flow conditions of airfoil swirl generator.

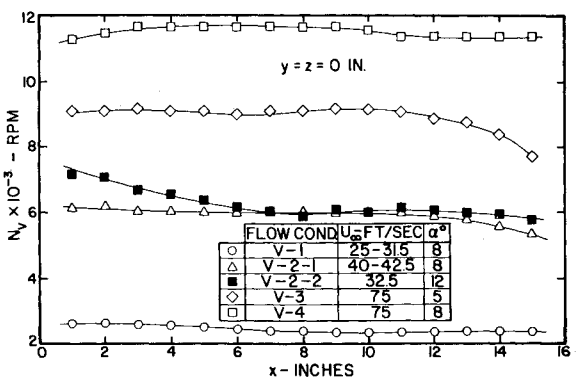

Fig. 3 Axial development of test flow conditions of airfoil swirl generator.

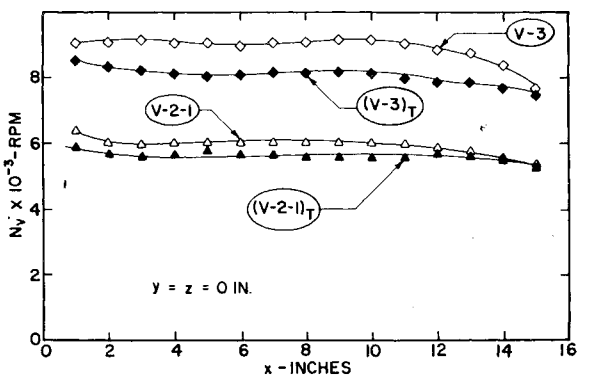

Fig. 5 Effect of upstream turbulence on airfoil test flow conditions.

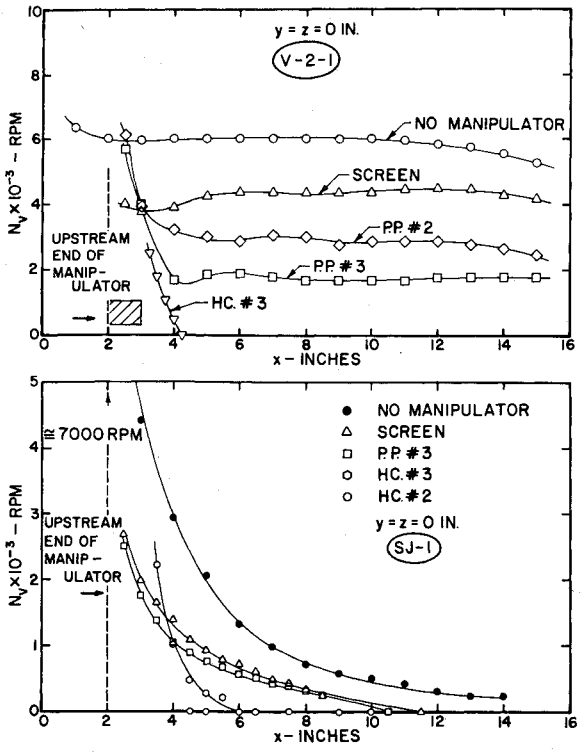

Fig. 6 Effect of various manipulators on downstream development of test flow conditions V-2-1 and SJ-1.

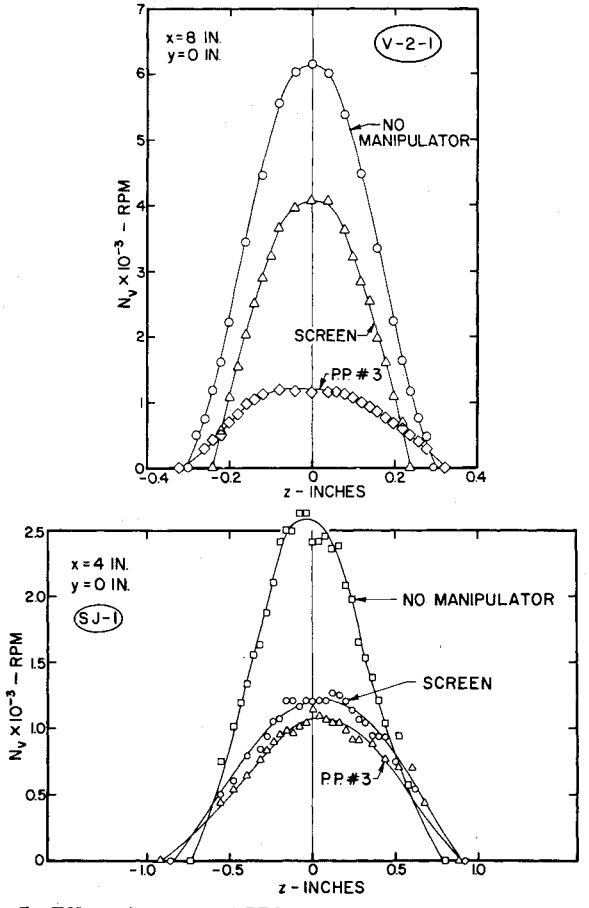

Fig. 7 Effect of screen and PP3 on vertical distribution of vorticity-indicator rotation in test flow conditions V-2-1 and SJ-1.

resulting output flows, as represented schematically in Fig. 1. The comparison of the flow downstream of any manipulator to the original test flow determined the effect of that manipulator on the flow condition. Such comparisons are shown for a variety of manipulators and two flow conditions in Fig. 6. The upper graph contains data on the downstream development of one of the airfoil swirl generator conditions, V-2-1, while the data in the lower graph are from a flow condition of the swirling-jet ejector, SJ-1. The top curve in each graph indicates the basic test flow condition and the other curves represent the flow downstream of specific flow manipulators as labeled. For discussion purposes, the flow manipulators used here are divided into two groups. One group contains screens, perforated plates, and other manipulators which have a characteristic mesh size, solidity, and a very short length, making them essentially two-dimensional. The other group contains manipulators such as honeycombs which have a substantial length, making the ℓ/d ratio an important parameter in addition to the mesh size and solidity. The mechanisms by which a manipulator modifies any swirling flow were different depending on these categories.

Concentrating first on screens and perforated plates, Fig. 6 shows that both remove some of the swirl, with the screen having less effect in flow condition V-2-1 than the perforated plate. In flow condition SJ-1, however, both manipulators have approximately the same effect. Note also that in flow condition V-2-1, the swirl intensity is not constant immediately downstream of the perforated plate but is constant downstream of the screen. The transverse distribution of the vorticity obtained from traverses parallel to these manipulators is shown in Fig. 7 for the same two flow conditions. In the lower graph, the traverses for the screen and perforated plate are very similar; however, in the upper graphs, the peak of the perforated plate traverse is not only much lower than that of the screen but also much flatter. To explain this apparent discrepancy, it is noted that the only major difference between these two flow conditions is the size of the swirling part of the flow, which is about three times larger in SJ-1, as shown by Fig. 7. The ratio of the mesh size of the manipulator to the characteristic size of the swirl is 2.5% and 22% for the screen and perforated plate, respectively, in the lower graphs of Figs. 6 and 7. In the upper graphs, the corresponding ratios are 6% and 55%. Based on these comparisons, one may surmise that the larger the mesh size in proportion to the size of the swirl, the greater the effectiveness of that manipulator in removing the swirl.

The explanation of this behavior is based on the presence of two mechanisms by which these manipulators remove such swirls from the flow. These mechanisms were suggested by the measurements previously described, as well as others made with X-wire probes in the same flows. The first mechanism is based on the idea of flow turning by screens.[2-4] The swirling flow enters the manipulator at some angle other than 90 deg due to its rotation and exits at an angle closer to 90 deg because of the turning effect, resulting in a corresponding decrease in the rotational speed of the flow. Immediately downstream of the manipulator, the swirling flow has the same form as the incoming flow; i.e., a concentrated vortex entering the manipulator leaves as a well-organized concentrated vortex. This mechanism is the dominant one as long as the mesh size is sufficiently smaller than the swirl size, as it is in the cases for the screen just shown.

As the mesh size approaches the swirl size for the same type of manipulator and solidity, the second mechanism begins to dominate. In this case, as the swirling flow is forced to pass through fewer openings in the grid, it usually becomes somewhat larger. The wakes from the solid part of the grid are also proportionately larger. While there is some turning of the flow corresponding to the first mechanism, it is the turbulent mixing of the wakes in this case which aids in the dissipation of the rotating part of the flow. The swirling flow leaving the manipulator consists of several regions of concentrated longitudinal vorticity separated by these wakes. As

Table 1 Properties of turbulence manipulators

	M, in.	σ	ℓ, in.	Re_M 25 fps	Re_M 50 fps	Re_M 75 fps
Screens:						
0.005 in. dacron thread	0.033	0.28	0.005	385	765	1150
0.007 in. stainless steel wire	0.0357	0.35	0.007	415	830	1240
Straws:						
Plastic 0.175 in. od and 0.006 in. wall	0.175	0.20	8.25	2030	4060	6090
Perforated plates:						
0.0625 in. steel PP2 0.14 in. holes	0.188	0.49	0.063	2180	4360	6540
PP3 0.25 in. holes	0.313	0.42	0.063	3630	7260	10890
Honeycomb:						
HC1 0.002 in. aluminum sheets 0.04 in. hexagon cell side	0.068	0.03	2 & 8	790	1580	2370
HC2 0.001 in. aluminum sheets 0.08 in. hexagon cell side	0.135	0.008	2	1570	3130	4700
HC3 0.0035 in. aluminum sheets 0.15 in. hexagon cell side	0.257	0.014	1	2980	5960	8950

these wakes spread into the rotating flow, the resulting flow again appears similar to the original test flow, but is of greatly diminished strength. This process requires some downstream distance to be completed and is demonstrated in Fig. 6 by the gradual decrease in the rotational speed beind the manipulator and its subsequent leveling off. This mechanism requires both a proper scaling of the manipulator mesh size to a characteristic size of the swirling part of the flow along with some turbulent mixing. Whether or not it is necessary to have a large amount of turbulence for this process is not yet known. Grids with larger meshes were also used in these flow conditions and found to remove the swirl entirely. In general, however, as the mesh size of the grid is increased, the generated turbulence also increases, so that separation of these two effects is not possible. On the other hand, it is conjectured that this concept of increasing the mesh size for better swirl removal has a limit. If the mesh size is too large, the swirl may pass completely through one opening in the grid and could exit with essentially no change.

As mentioned earlier, these mechanisms account for the behavior observed in perforated plates and screens, while different ones were found to dominate in the case of honeycombs. The effect of several honeycombs of different mesh sizes on these same two flow conditions is also shown in Fig. 6. Two of the honeycombs, HC1 and HC2, completely removed the measurable swirl within the manipulator itself. HC3 also removed all of the swirl from the flow, although not entirely within the manipulator. The differing behavior between these manipulators of the same type led to the conjecture that more than one mechanism was involved. Measurements with X-wire probes were again used to reveal them and document their details. Beginning with HC1 and HC2, as listed in Table 1, the mesh was too fine and the length too long for any of the incoming swirl to be present at the exit. The dominant mechanism here is the wall shear in each cell which effectively damps out the incoming vorticity. In the case of HC3, although all of the measurable swirl was removed, the mesh was too large and the length too short for wall shear to be the only effect. However, detailed measurements revealed that the flow downstream of HC3 did not resemble the incoming flow. Instead of one vortex, there was an array of vortices, all rotating in the same direction as the incoming vortex. These vortices scaled with the mesh size of the honeycomb rather than the incoming vortex. As this array progressed downstream, the regions of high shear between the vortices caused by their rotation were eliminated by the action of viscosity. This reduced the rotational speed of each of the vortices to such an extent that they were virtually removed. There was also evidence that two or more of the weakened vortices combined, but the details were not clear. This combination and elimination of the vortices explains the drop in rotational speed downstream of the honeycomb in the two flow conditions, as detected by the vane vorticity indicators and shown in Fig. 6.

This process is sensitive to the scaling of the mesh size to the swirl size as shown in Fig. 8. Flow conditions V-3 and V-4 of the airfoil swirl generator have the same freestream velocity with the vortex in flow condition V-4 being 50% larger and 30% stronger. Even though the vortex in flow condition V-4 is stronger, it decays faster due to its larger size and correspondingly greater number of weakened vortices downstream of the honeycomb. Figure 8 also emphasizes the ability of a manipulator to remove all of the measurable swirl from the flow, but not necessarily within the manipulator itself. This particular mechanism also proved to be very efficient in removing the swirl, as will be covered in Sec. IV.

In addition to the mechanisms for modifying the swirling flow, there are some other important results, which are best discussed with the aid of figures such as Fig. 9. Here, the swirl reduction ratio is plotted vs downstream distance for two manipulators and several flow conditions. Briefly, the swirl reduction ratio is defined as one minus the ratio of the rotational speed of the vane downstream of the manipulator to that at the same location in the basic test flow condition. It represents the percentage of swirl removed from the test flow condition, so that 100% swirl reduction means there is no measurable swirl left in the flow. In the top part of Fig. 9, the effect of a screen on all test flow conditions is plotted, with

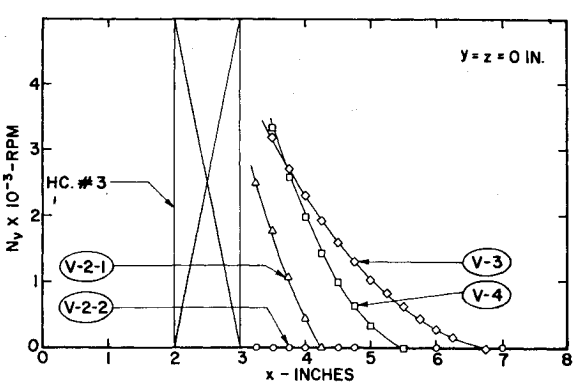

Fig. 8 Effect of HC3 on downstream development of several test flow conditions of airfoil swirl generator.

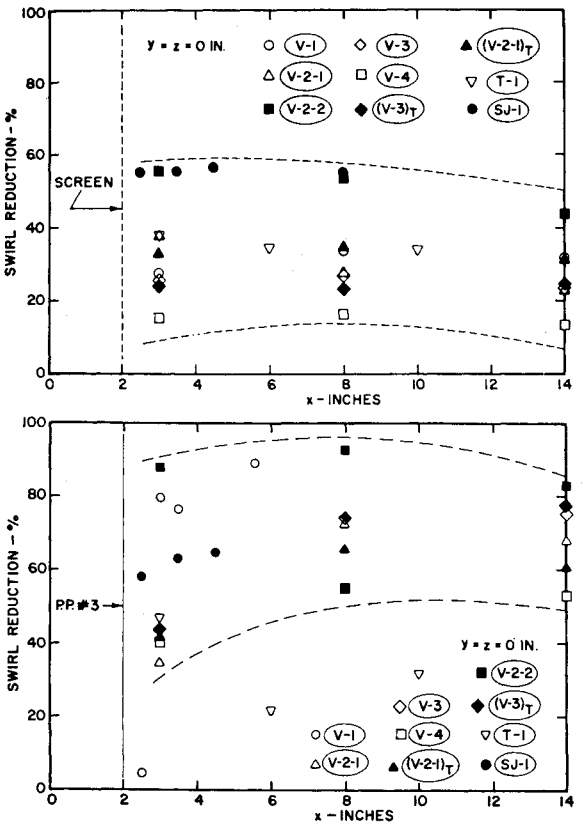

Fig. 9 Swirl reduction by screen and PP3 in various test flow conditions.

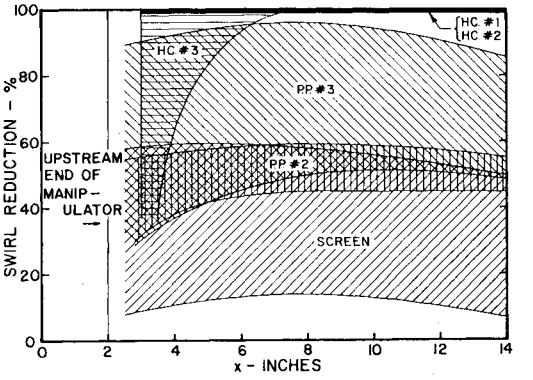

Fig. 10 Summary of swirl reduction by various manipulators in different test flow conditons.

the range indicated by the dashes. Similar results are plotted for PP3 (perforated plate) in the lower part of Fig. 9. These graphs indicate that not only does a manipulator cover a range of swirl reduction depending on the flow condition, but also that different manipulators cover different ranges.

The effect of background turbulence is also demonstrated using these graphs by comparing results for flow conditions V-2-1 and $(V\text{-}2\text{-}1)_T$ along with V-3 and $(V\text{-}3)_T$. There appears to be no difference in swirl reduction between flow conditions V-3 and $(V\text{-}3)_T$ for either manipulator. Considering flow conditions V-2-1 and $(V\text{-}2\text{-}1)_T$, the additional turbulence appears to aid in reducing the swirl downstream of the screen, but has the opposite effect downstream of PP3. However, the screen and PP3 operate with different mechanisms in flow condition V-2-1, as described earlier. Therefore, the effect of turbulence can be either favorable, unfavorable, or negligible, depending on the incoming flow conditions and the dominant swirl reduction mechanism. The details of the interaction have not yet been completely determined.

Reviewing results for flow conditions V-2-1 and V-2-2, which are flow conditions with the same strength vortices, but with the vortex in V-2-2 being much larger (as shown in Fig. 4), the corresponding reduction for both manipulators is greater for V-2-2 than for V-2-1. This demonstrates the importance of an appropriate scaling between the manipulator (e.g., its mesh and length) and the rotational part of the flow, not only for determining the dominant mechanism, but also for its effectiveness as well. The influence of the vortex strength on this process is exhibited in the results for flow conditions V-1 and V-3, which have vortices of the same size but of vastly different strengths. Both manipulators are found to be less effective as the vortex strength increases. This is supported by comparing flow conditions V-1, V-2-1, and V-4, which were generated using the same airfoil angle of attack but different freestream velocities, resulting in vortices of approximately the same size but again of different strengths.

Another interesting result is demonstrated by comparing flow conditions where these two effects are operating at the same time. Flow conditions V-3 and V-4 were generated at the same freestream velocity but the vortex for V-3 is smaller than that of V-4, (0.82 in. vs 1.22 in.), and is not as strong (9000 rpm vs 11,500 rpm). There is a greater swirl reduction of condition V-3 than for V-4 for both manipulators, which indicate that the difference in vortex strength outweighs the effect of the increased size of the vortex in V-4. However, in comparing flow conditions V-1 and V-2-2, again generated at the same freestream velocity, even though the vortex of V-2-2 is much larger than that of V-2-1 (1.56 in. vs 0.82 in.) and much stronger (6000 rpm vs 2500 rpm), we find that there is greater swirl reduction by both manipulators in flow condition V-2-2. In this case, the increased size outweighed the effect of the increased strength, which not only demonstrates the effect of proper scaling, but also that nonoptimized scaling can increase the importance of the other parameters, such as the vortex strength.

IV. Concluding Remarks

The effect of many parameters on the operation of some standard flow manipulators can be summarized as follows:

1) The effectiveness of a manipulator is reduced as the strength of the impinging swirl increases for the same size vortex and the same freestream velocity.

2) The reduction in swirl improves as the size of the vortex increases, for the same strength as long as the dominant mechanism for reducing the swirl stays the same.

3) Increasing the freestream turbulence level or its scale leads to more lateral diffusion of the swirl downstream of the manipulator. This enhances the operation of manipulators which do not generate much turbulence or significantly alter the shape and size of the swirling flow, as in the case of a screen. On the other hand, it disrupts the operation of manipulators which generate large amounts of turbulence, such as honeycombs[5] and perforated plates.[1] These manipulators operate through mechanisms which break the swirl into several parts that recombine downstream of the manipulator.

4) The pressure drop across the manipulator plays a minor or indirect role in the control of swirling flows.

5) For manipulators of the same mesh size, the effectiveness decrease as the solidity decreases.

These conditions outline some of the important considerations—notably that a manipulator should be scaled to the swirl size so that the mesh is not too large (which would allow the swirl to all go through one cell), nor too small (this would break the swirl up into too many small pieces). The experiments indicate that a mesh of approximately 20-25% the width of a concentrated swirl will give the best performance.

In order to use the conclusions about pressure drop and solidity, a look at the combined swirl reduction data for all

flow conditions and all manipulators is useful. A summary of these data is presented in Fig. 10, where the corresponding ranges of swirl reduction are shown for the different manipulators. The figure demonstrates the existence of overlapping regions, i.e., the same swirl reduction is obtainable with two different manipulators in comparable flow conditions. This would permit the selection of a manipulator based on other criteria, such as pressure drop coefficient or favorable turbulence control, which are desirable parameters to optimize.

Another interesting result which can be drawn from this figure is the behavior of the honeycombs. All of the honeycombs remove the swirl but by different mechanisms. The mechanism of HC1 and HC2 is to remove entirely any traces of the swirl totally within the manipulator. The mechanism of HC3 has been described in the last section, i.e., the elimination by effective recombination of the smaller, weakened swirls. The examples of HC1 and HC2 are those which were earlier referred to as "overkill," or the traditional way of doing things. Considering the pressure drop coefficients in Fig. 2, this is very costly indeed. For efficient operation, the length of the honeycomb required to completely remove the swirl is extremely short—less than four mesh lengths when the mesh is properly scaled to the swirl size. Use of such a honeycomb leads to great savings in energy due to its very low pressure drop coefficient.

Finally, while certain very short length, large mesh honeycombs are most efficient in removing swirl, the total picture is not that simple. Perforated plates, screens, and grids can be extemely useful in situations where turbulence control is a problem, where many scales of swirling flow exist, or where other basic mechanisms are present, such as shear at the wall of the duct. The large mesh honeycombs generate high levels of nonuniform turbulence, and with many sizes of swirl present, swirl reduction would not be as effective, due to the competing mechanisms within the same manipulator. In addition, other processes may hinder the effectiveness of its basic mechanism, e.g., rapid lateral diffusion caused by increased background turbulence.

Since recent studies[1,5] on the control of freestream turbulence show that rotational nonuniformities hinder the reduction of the turbulence, it is more efficient to work on the swirl first and then the turbulence. Since screens and perforated plates can take advantage of higher background turbulence for increased swirl reduction, in such flows a combination of one or more of these and a larger mesh honeycomb would be more efficient than using a longer, smaller mesh honeycomb. A family of properly spaced screens with decreasing mesh size (possibly in a variable area duct) may also be very effective.

Further studies are planned to investigate the effects of manipulators in tandem on simple and complex swirling flows. The ultimate goal of these studies is to provide detailed information and understanding which can be used to manage and manipulate swirling and secondary flows, as well as freestream turbulence, in a most efficient manner.

Acknowledgments

This research was supported by U.S. Army Research Office Grant DAHC04-74-G-0160 monitored by R. E. Singleton. The authors express their appreciation to Valerie Mattioli for her expert typing of the manuscript.

References

[1] Loehrke, R. I. and Nagib, H. M., "Experiments on Management of Free-Stream Turbulence," AGARD Rept. 598, AD-749-891, 1972.

[2] Taylor, G. I. and Batchelor, G. K., "The Effect of Wire Gauze on Small Disturbances in a Uniform Stream," *Quarterly Journal of Mechanics and Applied Mathematics*, Vol. 2, No. 1, 1949, p. 1.

[3] Dryden, H. L. and Schubauer, G. B., "Appendix to the Effect of Wire Gauze on Small Disturbances in a Uniform Screen," *Quarterly Journal of Mechanics and Applied Mathematics*, Vol. 2, No. 1, 1949, p. 1.

[4] Laws, E. M. and Livesey, J. L., "Flow Through Screens," *Annual Review of Fluid Mechanics*, Vol. 10, 1978, p. 247.

[5] Loehrke, R. I. and Nagib, H. M., "Control of Free-Stream Turbulence by Means of Honeycombs: A Balance Betwen Suppression and Generation," *Journal of Fluid Engineering*, Vol. 98, No. 3, 1976, p. 342.

[6] Ahmed, M., Wigeland, R. A., and Nagib, H. M., "Generation and Management of Swirling Flows in Confined Streams," Illinois Inst. of Technology, Fluids and Heat Transfer Rept. R76-2, 1976, AD A029 418.

[7] Holdeman, J. D. and Foss, J. F., "The Initiation, Development and Decay of the Secondary Flow in a Bounded Jet," *Journal of Fluid Engineering*, Vol. 97, No. 3, 1975, p. 342.

[8] McCormick, B. W., Tangler, J. L., and Sherrieb, H. E., "Structure of Trailing Vortices," *Journal of Aircraft*, Vol. 5, March 1968, p. 260.

[9] Barlow, J. B., "Measurements of Wing Wake Vorticity for Several Spanwise Load Distributions," University of Maryland Rept., 1972.

[10] Zalay, A. D., "Hot-Wire and Vorticity Meter Wake Vortex Surveys," *AIAA Journal*, Vol. 14, May 1976, p. 694.

[11] Wigeland, R. A., Ahmed, M., and Nagib, H. M., "Vorticity Measurements Using Calibrated Vane-Vorticity Indicators and Comparison with *X*-Wire Data," AIAA Paper No. 77-720, Albuquerque, New Mex., June 1977 (to appear in *AIAA Journal*).